Atmos. Chem. Phys. Discuss., https://doi.org/10.5194/acp-2017-1152
Manuscript under review for journal Atmos. Chem. Phys.
Discussion started: 15 December 2017


Atmospheric Chemistry and Physics Discussions

# African volcanic emissions influencing atmospheric aerosol particles over the Amazon rain forest

Jorge Saturno[1], Florian Ditas[1], Marloes Penning de Vries[1], Bruna A. Holanda[1], Mira L. Pöhlker[1], Samara Carbone[2,3], David Walter[1], Nicole Bobrowski[4,1], Joel Brito[2,5], Xuguang Chi[6], Alexandra Gutmann[7], Isabella Hrabe de Angelis[1], Luiz A. T. Machado[8], Daniel Moran-Zuloaga[1], Julian Rüdiger[9], Johannes Schneider[1], Christiane Schulz[1], Qiaoqiao Wang[10], Manfred Wendisch[11], Paulo Artaxo[2], Thomas Wagner[1], Ulrich Pöschl[1], Meinrat O. Andreae[1,12], and Christopher Pöhlker[1]

[1]Biogeochemistry, Multiphase Chemistry, and Particle Chemistry Departments, and Satellite Research Group, Max Planck Institute for Chemistry, P. O. Box 3060, 55020 Mainz, Germany
[2]Department of Applied Physics, Institute of Physics, University of São Paulo (USP), Rua do Matão, Travessa R, 187, CEP 05508-900, São Paulo, SP, Brazil
[3]Institute of Agrarian Sciences, Federal University of Uberlândia, Uberlândia, Minas Gerais, Brazil
[4]Institute for Environmental Physics, University of Heidelberg, Heidelberg, Germany
[5]Laboratory for Meteorological Physics, Université Clermont Auvergne, Clermont-Ferrand, France
[6]Institute for Climate and Global Change Research & School of Atmospheric Sciences, Nanjing University, Nanjing, 210093, China
[7]Department of Chemistry, Johannes Gutenberg University, Mainz, Germany
[8]Centro de Previsão de Tempo e Estudos Climáticos, Instituto Nacional de Pesquisas Espaciais, Cachoeira Paulista, Brazil
[9]Atmospheric Chemistry, University of Bayreuth, Dr.-Hans-Frisch-Straße 1–3, 95448 Bayreuth, Germany
[10]Institute for Environmental and Climate Research, Jinan University, Guangzhou, 511443, China
[11]Leipziger Institut für Meteorologie (LIM), Universität Leipzig, Stephanstr. 3, 04103 Leipzig, Germany
[12]Scripps Institution of Oceanography, University of California San Diego, La Jolla, CA 92098, USA

*Correspondence to*: Jorge Saturno (j.saturno@mpic.de) and Christopher Pöhlker (c.pohlker@mpic.de)

**Abstract.**

Long-range transport (LRT) plays an important role in the Amazon rain forest by bringing in different primary and secondary aerosol particles from distant sources. The atmospheric oxidation of dimethyl sulfide (DMS), emitted from marine plankton, is considered an important sulfate source over the Amazon rain forest, with a lesser contribution from terrestrial soil and vegetation sulfur emissions. Volcanic sulfur emissions from Africa could be a source of particulate sulfate to the Amazonian atmosphere upon transatlantic transport but no observations have been published. By using satellite observations, together with ground-based and airborne aerosol particle observations, this paper provides evidence of the influence that volcanic emissions have on the aerosol properties that have been observed

Atmos. Chem. Phys. Discuss., https://doi.org/10.5194/acp-2017-1152
Manuscript under review for journal Atmos. Chem. Phys.
Discussion started: 15 December 2017




in central Amazonia. Under the volcanic influence, sulfate mass concentrations reached up to 3.6 µg $m^{-3}$ (hourly mean) at ground level, the highest value ever reported in the Amazon region. The hygroscopicity parameter was higher than the characteristic dry-season average, reaching a maximum of 0.36 for accumulation mode aerosol particles. Airborne measurements and satellite data indicated the transport of two different volcanic plumes reaching the Amazon Basin in September 2014 with a sulfate-enhanced layer at an altitude between 4 and 5 km. These observations show that remote volcanic sources can episodically affect the aerosol cycling over the Amazon rain forest and perturb the background conditions. Further studies should address the long-term effect of volcanogenic aerosol particles over the Amazon Basin by running long-term and intensive field measurements in the Amazon region and by monitoring African emissions and their transatlantic transport.

## 1 Introduction

Sulfate aerosol particles are produced in the atmosphere by oxidation of sulfur dioxide ($SO_2$), emitted by fossil fuel (FF) combustion, volcanic emissions, and by oxidation of DMS (Andreae and Rosenfeld, 2008). These particles scatter solar radiation and act as efficient cloud condensation nuclei (CCN) (Stevens and Feingold, 2009). Anthropogenic $SO_2$ emissions have increased over the 20th century to a maximum around the year 1980 and declined somewhat thereafter to around 100 Tg $SO_2$ per year, but they are still the most important source of sulfur to the atmosphere (Boucher et al., 2013; http://edgar.jrc.ec.europa.eu/overview.php?v=431, last accessed 6 Sep 2017). Volcanic emissions are the predominant natural source of $SO_2$ and account for about 5 % of total $SO_2$ emissions (Yang et al., 2017). Sulfur dioxide is oxidized in the atmosphere to gaseous sulfuric acid, which is quickly converted to sulfate aerosol particles (Chin et al., 1996; Reiner and Arnold, 1994). Volcanic sulfur emissions can account for 20 – 40 % of sulfate aerosol particle mass concentrations in the middle troposphere at 650 hPa (Chin and Jacob, 1996). Volcanic eruptions can change the atmospheric composition (gas and particle phase) drastically in large areas (Mather et al., 2003). Two prominent examples are the Pinatubo eruption in 1991 (Kirchner et al., 1999) and the 2014 – 2015 eruption of the Holuhraun volcano in Iceland (Ilyinskaya et al., 2017), where the emissions affected the cloud-drop effective radius



($r_{eff}$) while other cloud properties like the cloud optical depth and the cloud liquid water path remained unaffected (Malavelle et al., 2017; Yuan et al., 2011). Moreover, a connection between tropical volcanic explosive eruptions and El Niño-like events has been described recently (Khodri et al., 2017). Besides explosive-effusive eruptions, small eruptions and passive degassing account for relatively stable $SO_2$ fluxes (23.0 ± 2.3 Tg $yr^{-1}$, 2005–2015), and approximately one order of magnitude higher than explosive eruptive $SO_2$ fluxes (Carn et al., 2017). To what extent volcanic passive sulfur emissions can affect cloud properties is still debated (Ebmeier et al., 2014; Malavelle et al., 2017). There are several active volcanoes in Africa. The Nyamuragira-Nyiragongo neighboring volcanoes in the Democratic Republic of the Congo (DRC) were among the most persistent passively degassing volcanoes worldwide between 2004 and 2014, with around 150 days with detected degassing in 2014 and the highest average $SO_2$ index observed in the period 2004 – 2014 (Carn et al., 2016). The strong passive degassing activity of Nyamuragira starting in 2011 and culminating in a formation of a lava lake in late 2014 (Campion, 2014) lead to enhanced $SO_2$ emission from the Nyiragongo-Nyamuragira complex for several years (Bobrowski et al., 2017).

In the Amazon rain forest, biogenic sulfate aerosol is sustained by oceanic DMS emission, and to a lesser degree by hydrogen sulfide ($H_2S$), methanethiol (MeSH), and DMS emissions from soils and vegetation (Andreae and Andreae, 1988; Jardine et al., 2015; Martin et al., 2010). Occasional anthropogenic sulfur injections have been attributed to open biomass burning and fossil fuel combustion emissions, either from Brazil or, via LRT, from Africa (Andreae et al., 1990; Talbot et al., 1988). A recent study suggests that fossil fuel sources (e.g., ship traffic, power plants) do not significantly influence aerosol particles measured in the remote Amazon forest (Saturno et al., 2017) but can be important downwind of populated areas like Manaus, Brazil (Kuhn et al., 2010; Martin et al., 2016). Recent measurements during the South AMerican Biomass Burning Analysis (SAMBBA) campaign, which focused on biomass burning (BB) emissions, found no correlation between sulfate aerosol and various kinds of BB aerosol particles (Brito et al., 2014). On the other hand, aircraft observations of haze layers at 2 – 4 km altitude over the Amazon rain forest have shown high sulfate enrichment in comparison to the boundary layer and the free troposphere concentrations and indicated these haze layers to be linked to LRT of aerosol particles from Africa (Andreae et al., 1988; Holanda et al., 2017).



A modeled global sulfate source attribution study showed that southern Africa peak sulfate concentrations occur between June and August. For this three-month period, estimated emissions were 0.81 Tg S and decreased in the following three months to 0.66 Tg S (Yang et al., 2017).

Northeasterly and southeasterly trade winds (north and south of the inter-tropical convergence zone (ITCZ), respectively) are able to transport aerosols over large distances given the typically weak wet deposition in this latitude band (Wang et al., 2016). During the Amazonian dry season (August – November), the transport of African smoke from southern Africa savanna and shrubland fires is an important source of aerosol in addition to the emissions by regional fires in South America (Andreae et al., 1994). When the ITCZ shifts north in the dry season, south-east trade winds originating from southern Africa are more likely to reach the central Amazon rain forest. Even though the potential impact of transatlantic transport of volcanic sulfur emission has been suggested (Yang et al., 2017), no ground-based evidence has been reported previously in the literature concerning the impact of African volcanic sources.

In this paper, we present satellite observations that show volcanic $SO_2$ emissions in central Africa that have been transported over the South Atlantic Ocean and reach the Amazon rain forest after being oxidized to particulate sulfate. Satellite, airborne, and ground-based observations are used to show that volcanogenic sulfate can significantly affect the aerosol physical and optical properties over the Amazon Basin during the dry season.

## 2 Data and methods

### 2.1 Ground-based instrumentation

The ground-based aerosol data presented here have been collected at the Amazon Tall Tower Observatory (ATTO) site (called *T0a* in the GoAmazon2014/5 experiment, (Martin et al., 2016)), located in the Uatumã Sustainable Development Reserve, Amazonas, Brazil. Details about the ATTO site infrastructure, instrumentation and an overview of running measurements can be found elsewhere (Andreae et al., 2015). Figure 1 shows the ATTO site location and the place of the Nyamuragira



volcano in the DRC located at 1.41° S, 29.2° E, 3058 m a.s.l. The long-term measurements at ATTO started in 2012. A systematic backward trajectory (BT) analysis of air masses arriving at ATTO can be found in Pöhlker et al. (2017a). The ATTO aerosol measurements were taken on a triangular mast (02° 08.602' S, 59° 00.033' W, 130 m above sea level, a.s.l.) using a 25 mm diameter, 60 m high stainless steel tube with a laminar sampling flow rate of 30 L $min^{-1}$. The instruments were installed inside an air-conditioned container where the temperature was kept between 29 and 31 °C.

Equivalent black carbon ($BC_e$) mass concentrations, $M_{BCe}$, were calculated from absorption measurements by a multi-angle absorption photometer, MAAP (Model 5012, Thermo Electron Group, Waltham, USA). The details of the instrument are described elsewhere (Petzold and Schönlinner, 2004). The BC mass absorption cross-section (MAC) was retrieved from fitting MAAP absorption coefficients at 637 nm wavelength and refractory black carbon (rBC) mass concentrations measured by using a single-particle soot photometer (SP2) revision D (Droplet Measurement Technologies, Boulder, USA). Details of the technique can be found in Stephens et al. (2003). The MAC calculations are described in Saturno et al. (2017). Light scattering coefficients were measured using a three-wavelength integrating nephelometer (Aurora 3000, Ecotech Pty Ltd., Knoxfield, Australia). For details of the instrument, see Müller et al. (2011). Absorption and interpolated scattering measurements at 637 nm wavelength were used to calculate the single scattering albedo of dry aerosol particles, $\omega_0$, at this wavelength, which is defined as the ratio of scattering to extinction coefficients (extinction = scattering + absorption). A detailed study of aerosol optical properties measured at the ATTO site can be found in Saturno et al. (2017).

An aerosol chemical speciation monitor (ACSM) (Aerodyne Research Inc., Billerica, USA) was used to measure online non-refractory aerosol chemical composition (Carbone et al., 2017). These measurements started in February 2014 at the ATTO site. The technique resolves the sub-micron aerosol chemical species in the following categories: Organics, sulfate, nitrate, ammonium and chloride (Ng et al., 2011). In this paper, we only use organics and sulfate mass concentration data, $M_{org}$ and $M_{sulfate}$, respectively.



Cloud condensation nuclei (CCN) number concentrations, $N_{CCN}$, were measured with a CCN counter (CCNC, model CCN-100, Droplet Measurement Technologies, Boulder, USA), which was deployed at the ATTO site starting in March 2014. The instrument scanned over a range of different supersaturations and particle diameters; more details can be found elsewhere (Pöhlker et al., 2016). The hygroscopicity parameter, $\kappa$, retrieved for a CCN activation ratio of 50 % is used in this study. Condensation nuclei number concentrations (> 10 nm), $N_{CN}$, were measured with a condensation particle counter (CPC, model 3022A, TSI, USA).

### 2.2 Airborne *in-situ* measurements

Chemical species of sub-micron aerosol particles were measured using a compact time-of-flight aerosol mass spectrometer (C-ToF-AMS) installed on board of the German High-Altitude and Long Range Research Aircraft (HALO, http://www.halo.dlr.de, last visited 13 September 2017), a modified business jet G550 (Gulfstream, Savannah, USA). The C-ToF-MS details are presented elsewhere (Drewnick et al., 2005). The measurements took place between 6 September and 1 October 2014, during the "Aerosol, Cloud, Precipitation, and Radiation Interactions and Dynamics of Convective Cloud Systems" (ACRIDICON) - "Cloud Processes of the Main Precipitation Systems in Brazil: A Contribution to Cloud Resolving Modeling and to the GPM (Global Precipitation Measurement)" (CHUVA) campaign over the Amazon rain forest (Machado et al., 2014). More details on the flight trajectories and instrumentation can be found elsewhere (Wendisch et al., 2016). In this study, only data up to 7 km altitude have been used.

### 2.3 Air mass trajectories

To investigate the probability of the volcanic sulfate plume reaching the ATTO site, trajectories were calculated using the National Oceanic and Atmospheric Administration (NOAA) hybrid single-particle Lagrangian integrated trajectory HYSPLIT model (Draxler and Hess, 1997, 1998; Stein et al., 2015). NOAA Global Data Assimilation System (GDAS) (Kleist et al., 2009) data at 1° × 1° resolution were used as meteorological input for HYSPLIT.

Atmos. Chem. Phys. Discuss., https://doi.org/10.5194/acp-2017-1152
Manuscript under review for journal Atmos. Chem. Phys.
Discussion started: 15 December 2017




### 2.4 Satellite $SO_2$ VCD data

As one of the most abundant gases in a volcanic plume, $SO_2$ is often used as a tracer for volcanic emissions by a variety of spectroscopic remote sensing techniques. The strong characteristic absorption features in the UV spectral range allow the quantification of $SO_2$ using differential optical absorption spectroscopy (DOAS, see e.g. Platt and Stutz, 2008; Richter and Wagner, 2011), both from the ground (e.g. Bobrowski and Platt, 2007; Galle et al., 2003) and from space (e.g., Eisinger and Burrows, 1998; Khokhar et al., 2005; Krueger and J., 1985).

The ozone monitoring instrument (OMI) on board of the National Aeronautics and Space Administration (NASA) Aura satellite, launched in 2004, detects backscattered solar radiation in the UV-visible range (Levelt et al., 2006). The polar-orbiting instrument crosses the equator at 13:30 local time. DOAS analysis of OMI spectra yields column densities of trace gases such as $NO_2$, $SO_2$, and HCHO with a spatial resolution of about $13 \times 24$ km$^2$ away from the swath edges. OMI's wide swath of 2600 km allowed daily global coverage until the first occurrence of the so-called row anomaly in June 2007, an instrumental problem that causes grievous radiance errors in up to half of OMI's ground pixels (Van Hoek and Claas, 2010). The row anomaly strongly affects the reliability of observations; therefore all affected pixels were removed from the data set prior to analysis.

The OMI $SO_2$ vertical column density (VCD) data presented in this paper were retrieved using the NASA's principal-component based algorithm with an a-priori vertical profile representative of a volcanic plume in the middle troposphere (TRM, Li et al., 2013, 2017). The assumption that the volcanic plume is located in the mid–troposphere is justified by the elevation of the volcano (3 km), the strength of the eruption, and, particularly, the HYSPLIT trajectory analysis presented later in this paper. It is, however, important to note that the sensitivity of the satellite measurements depends systematically on plume altitude. Thus, the absolute values of the $SO_2$ VCD derived from the satellite observations over- or underestimate the true values if the plume is located at a higher or lower altitude, respectively. Fortunately, this does not influence our study, as the focus of this paper is on the spatial pattern of the $SO_2$ plumes, and not on $SO_2$ amount.



The level-2 data were downloaded from: https://mirador.gsfc.nasa.gov/ (last visited 27 October 2017) and gridded to a regular, 0.1° × 0.1° grid for easily handling.

Multi-year OMI $SO_2$ VCD daily averages from 11° S to 17° N are summarized in Fig. S1 as a function of time and longitude. The figure shows observations during the ATTO measurement period (March 2012 to July 2017) and a snapshot of September 2014. Given that the Nyamuragira and Nyiragongo volcanoes are so close to each other (within ~15 km), their emissions detected by remote sensors are often treated as a paired source (Carn et al., 2017). Hereafter, the term "Nyamuragira" refers to the couple Nyamuragira-Nyiragongo in this text. Time series of area-averaged OMI $SO_2$ observations are shown in Fig. 2a. Nyamuragira produced frequent intensive $SO_2$ emission events especially from 2012 to the end of 2015. The area where the average was calculated (Fig. 2b) corresponds to approximately 200,000 $km^2$ around Nyamuragira. Emissions from Nyamuragira were often transported westward, as can be observed in HYSPLIT forward trajectories calculated for 2014 (Fig. S2).

## 3 Results and discussion

### 3.1 Satellite measurements and trajectory analysis of the volcanic plume

The most important activity at the Nyamuragira volcano since 2011 occurred in September 2014 (Global Volcanism Program, 2017), coinciding with ground and airborne measurement campaigns in the Amazon Basin (Andreae et al., 2015; Wendisch et al., 2016; Martin et al., 2017). Satellite $SO_2$ VCD observations over central Africa and the Atlantic Ocean were examined during this period in order to precisely identify the volcanic eruptive period and the plume trajectory. A map of gridded OMI $SO_2$ TRM VCD observations from 7 to 17 September 2014, is available as supplementary material (Fig. S3). Two important emission events were observed at the Nyamuragira location, one on 7 September and another on 12 September. The latter one exhibits a clear westward transport of the $SO_2$ plume starting from 13 to 17 September. Figure 3 shows $SO_2$ VCD observations during this period within the region between 20 W – 30 E, and 15 S – 5 N with $SO_2$ VCD larger than $2.5 \times 10^{16}$ molecules $cm^{-2}$. Several sets of trajectory calculations were performed. First, three to seven starting locations were selected within



the $SO_2$ plumes detected by OMI on 12–17 September 2014. At each location, 15-day (360 hours) forward trajectories were started at the time of the satellite overpass (11 – 14 UTC) at seven altitudes spaced equally between 1 and 7 km. The resulting trajectories initialized at 4 km altitude on 13 September are in best agreement with the satellite data and are shown in Fig. 3. All starting parameters were systematically varied and very consistent patterns were found. The trajectories are superimposed on the map presenting all $SO_2$ plumes detected by OMI between 12 and 17 September. Trajectories started within the leading edge of the plume are in good agreement with the OMI data, as after 24 hours (second marker) both trajectories are located within the plume detected on 14 September, and after 48 hours (third marker) both trajectories are located within the plume detected on 15 September. The two southernmost trajectories make a sharp turn after 15 September, which is in agreement with the observed pattern, although there is no longer an exact match with the respective OMI observations (in red and maroon). This discrepancy may be due to inaccuracy of the individual trajectories, or the $SO_2$ plumes might have been below OMI's detection limit. The southernmost trajectories reach South America and come within several hundreds of kilometers of ATTO within 15 days. One of them reached ATTO on 25 September at 1.8 km altitude, whereas the other one passed at an altitude of 1.5 km at the point nearest to ATTO on 24 September.

In addition to the plume forward trajectory analysis, backward trajectories initiated at the ATTO site at an altitude of 300 m (approximately 170 m above ground) were calculated for 360 hours. These trajectories were initiated every hour from 20 September 0:00 UTC up to 30 September 23:00 UTC. The results, presented as a trajectory density plot in Fig. 4, indicate that although during this time period essentially all air masses come from southern Africa, they usually come from further south. Nevertheless, a significant number of trajectories originates close to the volcano and its plume.

### 3.2 Airborne observation of the volcanogenic aerosol particles

Enhanced sulfate aerosol mass concentrations were observed above 3 km height over the Amazon Basin during the ACRIDICON-CHUVA campaign compared to lower altitudes. A map including all airborne observations on the different flights can be found in the supplementary material (Fig. S4). However, given the multiple sulfate aerosol sources, sulfate itself can not be used as a tracer of volcanic



emissions. In order to distinguish the volcanogenic sulfate from additional aerosol sources like BB, which is important during this time of the year, we examined the $M_{sulfate}$ vertical profiles together with their sulfate-to-OA mass ratio ($M_{sulfate}$ / $M_{org}$). A list of the ACRIDICON-CHUVA flights and $M_{sulfate}$ vertical profiles are presented as supplementary information in Table S1 and Fig. S5, respectively. From the different airborne observations, flight AC14 showed the highest sulfate-to-OA mass ratio, indicating the strongest volcanogenic influence. The $M_{sulfate}$ vertical profile measured on 21 September 2014 (AC14) is presented in Fig. 5. The observations show a sulfate-enhanced layer between 4 and 5 km height. The average $M_{sulfate}$ observed during flight AC14 was 1.1 ± 0.5 µg m$^{-3}$ between 3 and 6 km height. This sulfate-enhanced layer exhibits a sulfate-to-OA ratio generally larger than 1. It can be distinguished from lower layers, below 3 km height, which are characteristically rich in OA due to BB and biogenic emissions. Usually, BB aerosol particles have been shown to have higher OA mass concentrations than other aerosol particles (McNaughton et al., 2011; Saturno et al., 2017). Therefore, the high sulfate-to-OA ratio is an indication of the volcanic origin of the probed aerosol. Backward trajectories were calculated from several points along the flight paths. Figure 6 shows backward trajectories started at nine points along the AC14 flight track where sulfate-to-OA ratios larger (colored lines) or smaller than 1 (gray lines) were detected; the flight and aerosol data measured at each point are presented in Table 1. Figure 6 clearly shows that the (colored) trajectories, with one exception, initialized within the sulfate plume originate from central Africa, whereas the gray trajectories, started outside of the sulfate plume, appear to originate from South America or from more southern regions over or across the Atlantic Ocean. The air mass trajectory analysis indicates that the AC14 observations were likely the result of probing the volcanic plume emitted on 7 September, the first one detected by OMI (see Fig. S3). For flight AC17 a similar pattern is observed, with three out of four (colored) trajectories started within the sulfate plume originating from central Africa and half of the other trajectories clearly coming from regions more to the South (see supplement, Fig. S6 and Table S2).

Figures 3, 4, and 6 show that the trajectories agree well, but not perfectly with the ground-based, airborne, and satellite measurements, which is mainly caused by the uncertainty of such long trajectories. Nevertheless, the fact that forward and backward trajectories calculated from various starting points and times agree on the sulfate source is a strong indication that the sulfate plumes

Atmos. Chem. Phys. Discuss., https://doi.org/10.5194/acp-2017-1152
Manuscript under review for journal Atmos. Chem. Phys.
Discussion started: 15 December 2017




observed at and near ATTO originate from the Nyamuragira volcano. Combined with the westward transport pattern derived from $SO_2$ satellite data and the lack of an alternative strong sulfate source makes this a quite convincing case.

### 3.3 Volcanic emission effects on the aerosol particle properties

The arrival of the African volcanic emissions over the Amazon rain forest affected the aerosol physical and chemical properties measured at the ATTO site. The most evident effect was the significant increase in $M_{sulfate}$. The 90$^{th}$ percentile of $M_{sulfate}$ measured at the ATTO site during the dry season 2014 was used as a threshold to define the volcanic influence event (Nya2014) as the time when this threshold was exceeded. By this criterion, the Nya2014 event spanned from 21 September 2014 at 02:00 UTC to 1 October 2014 at 01:00 UTC. Figure 7 shows different aerosol parameters measured before, during and after the Nya2014 event. The $N_{CN}$, shown in Fig. 7a, did not vary greatly from the values typical of the season (Pöhlker et al., 2016). The average $N_{CN}$ during the dry season in 2014 was $(1.3 \pm 0.6) \times 10^3$ particles cm$^{-3}$, whereas during the Nya2014 event, there were three peaks lasting for few hours with particle number concentrations higher than $3.0 \times 10^3$ particles cm$^{-3}$ on 27, 29, and 30 September 2014.

During the Nya2014 period, $M_{sulfate}$ averaged $1.7 \pm 0.6$ µg m$^{-3}$, which was significantly above the dry season 2014 average of $0.7 \pm 0.3$ µg m$^{-3}$, see Fig. 7b. The highest $M_{sulfate}$ value observed at the ATTO site was 3.6 µg m$^{-3}$ (hourly mean) on 26 September 2014. For comparison, during the SAMBBA campaign in southern Amazonia, $M_{sulfate}$ barely exceeded 1.0 µg m$^{-3}$, despite organics nearly reaching 100 µg m$^{-3}$, $M_{BCe}$ of 5 µg m$^{-3}$ and $N_{CN}$ above $25 \times 10^3$ particles cm$^{-3}$ during the peak of biomass burning (Brito et al., 2014). A long-term measurement study, also conducted in southern Amazonia, reported $M_{sulfate}$ of $1.1 \pm 0.7$ µg m$^{-3}$ during the dry season, with a maximum of 3.3 µg m$^{-3}$ for aerosol particles with mobility diameters smaller than 2 µm (Artaxo et al., 2002). It is important to note that Artaxo et al.'s (2002) sulfate observations were done under strong BB influence with average elemental carbon (EC) mass concentrations, $M_{EC}$, of $3.8 \pm 4.2$ µg m$^{-3}$, with a maximum of 25 µg m$^{-3}$. In contrast, the $BC_e$ measurements at the ATTO site during the Nya2014 event had an average of $0.4 \pm 0.1$ µg m$^{-3}$, with a maximum of 0.8 µg m$^{-3}$, indicating that the BB influence was relatively weak during the period of

Atmos. Chem. Phys. Discuss., https://doi.org/10.5194/acp-2017-1152
Manuscript under review for journal Atmos. Chem. Phys.
Discussion started: 15 December 2017




interest, with some short (few hours) spikes due to the influence of near-by fire events, see Fig. 7b. At a sampling site impacted by Manaus emissions, the sub-micron $M_{sulfate}$ was about 0.2 µg m$^{-3}$ during the wet season, rarely exceeding 0.6 µg m$^{-3}$ (de Sá et al., 2017). Therefore, even considering a range of pollution sources, our measurements at ATTO during the Nya2014 event are the highest sub-micron sulfate concentration ever reported in the Amazon Basin; see Martin et al. (2010) for a summary of wet and dry season aerosol observations. For comparison, the ACRIDICON-CHUVA airborne measurements are also included in Fig. 7b. The $M_{sulfate}$ measured on flight AC14 was significantly enhanced between 3 to 6 km altitude, reaching a median of 1.0 µg m$^{-3}$ and a 75$^{th}$ percentile of 1.6 µg m$^{-3}$. Previous aircraft measurements during the SAMBBA campaign reported a $M_{sulfate}$ flight average of 0.48 µg m$^{-3}$ (Allan et al., 2014).

The increased $M_{sulfate}$ period was accompanied by an enhanced sulfate-to-OA mass ratio, according to the ATTO observations (Fig. 7c). The Ny2014 sulfate-to-OA average over about 10 days was 0.38 ± 0.09, significantly higher than the dry season average of 0.18 ± 0.15. During some BB pulses, decreased sulfate-to-OA ratios were observed, but the whole Nya2014 period was exceptionally high compared to the typical dry season conditions. The sulfate-to-OA values measured at ground level were usually lower than the airborne values observed between 3 and 6 km height because the OA sources (BB and biogenic emissions) are located at ground level and the LRT sulfate that arrives at higher altitudes is diluted upon vertical mixing. The possibility of fossil-fuel (FF) burning was ruled out as an important sulfur source during the event discussed here because of the particularly high dry-aerosol $\omega_0$ measured during the event (0.89 ± 0.04), as can be observed in the color code data in Fig. 7c. Usually FF emissions, rich in BC, present characteristically low $\omega_0$ (0.2 – 0.3) (Bond and Bergstrom, 2006) and its addition would have lowered the value of $\omega_0$. Instead, an increase in $\omega_0$ was observed to values higher than 0.90 during the period of maximum $M_{sulfate}$ (26 – 27 September 2014).

The effects of the volcanic sulfur plume on the aerosol hygroscopicity was explored by analyzing the $\kappa$ values measured at different supersaturations. Higher $\kappa$ values were measured for the accumulation mode aerosol (particles with diameter greater than 100 nm) (Fig. 7d; note the color-coded particle activation diameter, $D_a$). During the Nya2014 event, the $\kappa$ values increased significantly, especially when the maximum $M_{sulfate}$ was observed. For example, the average $\kappa$ for a supersaturation of 0.10 %



($D_a$ = 167 – 179 nm, 25th and 75th percentile, respectively) was 0.26 ± 0.04 during the Nya2014 event, with a maximum of 0.36. The Nya2014 $\kappa$ average was slightly higher than the 2014 dry season average of 0.21 ± 0.03 for 0.10 % supersaturation (excluding the volcanic event), and significantly higher than a strong BB event average of 0.18 ± 0.01 for 0.10 % supersaturation, whose high OA content (sulfate-to-OA < 0.04) caused a significant drop in the hygroscopicity parameter (Pöhlker et al., 2017b).

## Summary and conclusions

Satellite $SO_2$ observations showed two explosive events at the Nyamuragira volcano on 7 and 12 September 2014. These emissions were observed to be transported over the South Atlantic Ocean. Air mass trajectory modeling from the plume location showed that the plume was transported towards South America, likely over the ATTO site and its surroundings in central Amazonia. Airborne observations during the ACRIDICON-CHUVA campaign showed a sulfate-enhanced layer between 4 and 5 km height on 21 September 2014 (flight AC14). Additionally, this layer exhibited an increased sulfate-to-OA mass ratio with medians higher than 1 for measurements between 3 and 6 km height.

The ground-based $M_{sulfate}$ measured at the ATTO site reached an hourly mean of 3.6 µg $m^{-3}$ on 26 September 2014, the highest values ever reported in the Amazon Basin. The sulfate-to-OA mass ratio increased from a dry-season average of 0.18 ± 0.15 to 0.38 ± 0.09 during the volcanic influence event, which spanned for a period of about 10 days. Increased sulfate-to-OA and single scattering albedo ($\omega_0$) were assumed as an indication of the low influence of BB and FF sources, respectively. In terms of aerosol hygroscopicity, the values of $\kappa$ (for 0.10 % supersaturation) measured during the volcanic event reached an average of 0.26 ± 0.04 (and a maximum of 0.36), slightly higher than the dry season average of 0.21 ± 0.03.

The evidence presented here shows one particular event of volcanic $SO_2$ emissions in Africa influencing the aerosol particles' chemical composition, hygroscopicity, and optical properties in the Amazon Basin. Therefore, our study indicates that these emissions and their transatlantic transport could potentially affect the Amazonian cloud microphysical properties. However, the extent and relevance of the episodic volcanic influence on the Amazonian atmosphere would require more extensive studies. Beyond the



effects and implications of this particular event, the results of our study represent a reference case of the dynamics and conditions of transatlantic aerosol transport from southern Africa to South America. This could help to understand the inter-continental advection of other aerosol species, such as combustion aerosol particles that are more difficult to trace.

*Data availability*. The data presented in this paper can be accessed via e-mail request to Jorge Saturno (j.saturno@mpic.de) or Christopher Pöhlker (c.pohlker@mpic.de). OMI data are available online at https://disc.gsfc.nasa.gov/.

*Competing interests.* The authors declare that they have no conflict of interest.

## Acknowledgements

This work has been supported by the Max Planck Society (MPG) and the Paul Crutzen Graduate School (MPGS). For the operation of the ATTO site, we acknowledge the support by the German Federal Ministry of Education and Research (BMBF contract 01LB1001A) and the Brazilian Ministério da Ciência, Tecnologia e Inovação (MCTI/FINEP contract 01.11.01248.00) as well as the Amazon State University (UEA), FAPEAM, LBA/INPA and SDS/CEUC/RDS-Uatumã. We acknowledge the generous support of the ACRIDICON-CHUVA campaign by the Max Planck Society, the German Aerospace Center (DLR), FAPESP (São Paulo Research Foundation), and the German Science Foundation (Deutsche Forschungsgemeinschaft, DFG). This study was also supported by EU Project HAIC under FP7-AAT-2012-3.5.1-1 and by the German Science Foundation within DFG SPP HALO by contract no VO1504/4-1 and contract no JU 3059/1-1. The ACRIDICON-CHUVA aircraft measurements presented here were supported by BMBF, grant No. 01LG1205E (ROMIC-SPITFIRE) and by DFG (SCHN1138/1-2). This paper contains results of research conducted under the Technical/Scientific Cooperation Agreement between the National Institute for Amazonian Research, the State University of Amazonas, and the Max-Planck-Gesellschaft e.V.; the opinions expressed are the entire responsibility of the authors and not of the participating institutions. We highly acknowledge the support by the Instituto Nacional de Pesquisas da Amazônia (INPA). We would like to especially thank all the people involved in the technical, logistical, and scientific support of the ATTO project, in particular Reiner Ditz, Jürgen Kesselmeier, Alberto Quesada, Niro Higuchi, Susan Trumbore, Matthias Sörgel, Thomas Disper, Andrew Crozier, Uwe Schulz, Steffen Schmidt, Antonio Ocimar Manzi, Alcides Camargo Ribeiro, Hermes Braga Xavier, Elton Mendes da Silva, Nagib Alberto de Castro Souza, Adi Vasconcelos Brandão, Amaury Rodrigues Pereira, Antonio Huxley Melo Nascimento, Feliciano de Souza Coehlo, Thiago de Lima Xavier, Josué Ferreira de Souza, Roberta Pereira de Souza, Bruno Takeshi, and Wallace Rabelo Costa. J. Saturno thanks the PhD scholarship funding from Fundación Gran Mariscal de Ayacucho (Fundayacucho) and acknowledges Loreto Donoso, Martin Brüggemann, and David Cabrera for support and stimulating discussions. Moreover, we appreciate the support by Jošt V. Lavrič, Tobias Könemann,

Luciana V. Rizzo, Henrique M. Barbosa, Patrick Schlag, Florian Dinger, Hang Su, Yafang Cheng, and Stephan Borrmann. We thank the GoAmazon2014/5 team, in particular Scot T. Martin. We also thank the ACRIDICON-CHUVA campaign team.

We acknowledge the NOAA Air Resources Laboratory (ARL) for the provision of the HYSPLIT transport and dispersion model and READY website (http://www.ready.noaa.gov) used in this publication. We also acknowledge NASA for providing the OMI/$SO_2$ total column level 2 data available online by the Goddard Earth Sciences Data and Information Services Center (GES DISC).

Atmos. Chem. Phys. Discuss., https://doi.org/10.5194/acp-2017-1152
Manuscript under review for journal Atmos. Chem. Phys.
Discussion started: 15 December 2017




## References

Allan, J. D., Morgan, W. T., Darbyshire, E., Flynn, M. J., Williams, P. I., Oram, D. E., Artaxo, P., Brito, J., Lee, J. D. and Coe, H.: Airborne observations of IEPOX-derived isoprene SOA in the Amazon during SAMBBA, Atmos. Chem. Phys., 14(20), 11393–11407, doi:10.5194/acp-14-11393-2014, 2014.

Andreae, M. O. and Andreae, T. W.: The cycle of biogenic sulfur compounds over the Amazon Basin: 1. Dry season, J. Geophys. Res., 93(D2), 1487, doi:10.1029/JD093iD02p01487, 1988.

Andreae, M. O. and Rosenfeld, D.: Aerosol–cloud–precipitation interactions. Part 1. The nature and sources of cloud-active aerosols, Earth-Science Rev., 89(1–2), 13–41, doi:10.1016/j.earscirev.2008.03.001, 2008.

Andreae, M. O., Browell, E. V., Garstang, M., Gregory, G. L., Harriss, R. C., Hill, G. F., Jacob, D. J., Pereira, M. C., Sachse, G. W., Setzer, A. W., Dias, P. L. S., Talbot, R. W., Torres, A. L. and Wofsy, S. C.: Biomass-burning emissions and associated haze layers over Amazonia, J. Geophys. Res., 93(D2), 1509, doi:10.1029/JD093iD02p01509, 1988.

Andreae, M. O., Berresheim, H., Bingemer, H., Jacob, D. J., Lewis, B. L., Li, S.-M. and Talbot, R. W.: The atmospheric sulfur cycle over the Amazon Basin: 2. Wet season, J. Geophys. Res., 95(D10), 16813, doi:10.1029/JD095iD10p16813, 1990.

Andreae, M. O., Anderson, B. E., Blake, D. R., Bradshaw, J. D., Collins, J. E., Gregory, G. L., Sachse, G. W. and Shipham, M. C.: Influence of plumes from biomass burning on atmospheric chemistry over the equatorial and tropical South Atlantic during CITE 3, J. Geophys. Res., 99(D6), 12793, doi:10.1029/94JD00263, 1994.

Andreae, M. O., Acevedo, O. C., Araùjo, A., Artaxo, P., Barbosa, C. G. G., Barbosa, H. M. J., Brito, J., Carbone, S., Chi, X., Cintra, B. B. L., da Silva, N. F., Dias, N. L., Dias-Júnior, C. Q., Ditas, F., Ditz, R., Godoi, A. F. L., Godoi, R. H. M., Heimann, M., Hoffmann, T., Kesselmeier, J., Könemann, T., Krüger, M. L., Lavric, J. V, Manzi, A. O., Lopes, A. P., Martins, D. L., Mikhailov, E. F., Moran-Zuloaga, D., Nelson, B. W., Nölscher, A. C., Santos Nogueira, D., Piedade, M. T. F., Pöhlker, C., Pöschl, U., Quesada, C. A., Rizzo, L. V, Ro, C.-U., Ruckteschler, N., Sá, L. D. A., de Oliveira Sá, M., Sales, C. B., dos Santos, R. M. N., Saturno, J., Schöngart, J., Sörgel, M., de Souza, C. M., de Souza, R. A. F., Su, H., Targhetta, N., Tóta, J., Trebs, I., Trumbore, S., van

Eijck, A., Walter, D., Wang, Z., Weber, B., Williams, J., Winderlich, J., Wittmann, F., Wolff, S. and Yáñez-Serrano, A. M.: The Amazon Tall Tower Observatory (ATTO): Overview of pilot measurements on ecosystem ecology, meteorology, trace gases, and aerosols, Atmos. Chem. Phys., 15(18), 10723–10776, doi:10.5194/acp-15-10723-2015, 2015.

Artaxo, P., Martins, J. V., Yamasoe, M. A., Procópio, A. S., Pauliquevis, T. M., Andreae, M. O., Guyon, P., Gatti, L. V. and Cordova Leal, A. M.: Physical and chemical properties of aerosols in the wet and dry seasons in Rondônia, Amazonia, J. Geophys. Res., 107(D20), 8081, doi:10.1029/2001JD000666, 2002.

Bobrowski, N. and Platt, U.: SO2/BrO ratios studied in five volcanic plumes, J. Volcanol. Geotherm. Res., 166(3–4), 147–160, doi:10.1016/j.jvolgeores.2007.07.003, 2007.

Bobrowski, N., Giuffrida, G. B., Arellano, S., Yalire, M., Liotta, M., Brusca, L., Calabrese, S., Scaglione, S., Rüdiger, J., Castro, J. M., Galle, B. and Tedesco, D.: Plume composition and volatile flux of Nyamulagira volcano, Democratic Republic of Congo, during birth and evolution of the lava lake, 2014–2015, Bull. Volcanol., 79(12), 90, doi:10.1007/s00445-017-1174-0, 2017.

Bond, T. C. and Bergstrom, R. W.: Light Absorption by Carbonaceous Particles : An Investigative Review, Aerosol Sci. Technol., 40, 27–67, doi:10.1080/02786820500421521, 2006.

Boucher, O., Randall, D., Artaxo, P., Bretherton, C., Feingold, G., Forster, P., Kerminen, V.-M., Kondo, Y., Liao, H., Lohmann, U., Rasch, P., Satheesh, S. K., Sherwood, S., Stevens, B. and Zhang, X. Y.: Clouds and Aerosols, in Climate Change 2013 - The Physical Science Basis, edited by Intergovernmental Panel on Climate Change, pp. 571–658, Cambridge University Press, Cambridge., 2013.

Brito, J., Rizzo, L. V., Morgan, W. T., Coe, H., Johnson, B., Haywood, J., Longo, K., Freitas, S., Andreae, M. O. and Artaxo, P.: Ground-based aerosol characterization during the South American Biomass Burning Analysis (SAMBBA) field experiment, Atmos. Chem. Phys., 14(22), 12069–12083, doi:10.5194/acp-14-12069-2014, 2014.

Campion, R.: New lava lake at Nyamuragira volcano revealed by combined ASTER and OMI SO2 measurements, Geophys. Res. Lett., 41(21), 7485–7492, doi:10.1002/2014GL061808, 2014.

Carbone, S., Brito, J. F., Xu, L., Ng, N. L., Rizzo, L. V., Stern, R., Cirino, G. G., Holanda, B. A., Senna, E., Wolff, S., Saturno, J., Chi, X., Souza, R. A. F., Arana, A., de Sá, M., Pöhlker, M. L., Andreae, M. O., Pöhlker, C., Barbosa, H. M. J. and Artaxo, P.: Long-term chemical composition and source apportionment of submicron aerosol particles in the central Amazon basin (ATTO), Atmos. Chem. Phys. Discuss., in preparation, 2017.



Carn, S. A., Clarisse, L. and Prata, A. J.: Multi-decadal satellite measurements of global volcanic degassing, J. Volcanol. Geotherm. Res., 311, 99–134, doi:10.1016/j.jvolgeores.2016.01.002, 2016.

Carn, S. A., Fioletov, V. E., McLinden, C. A., Li, C. and Krotkov, N. A.: A decade of global volcanic SO2 emissions measured from space, Sci. Rep., 7, 44095, doi:10.1038/srep44095, 2017.

Chin, M. and Jacob, D. J.: Anthropogenic and natural contributions to tropospheric sulfate: A global model analysis, J. Geophys. Res. Atmos., 101(D13), 18691–18699, doi:10.1029/96JD01222, 1996.

Chin, M., Jacob, D. J., Gardner, G. M., Foreman-Fowler, M. S., Spiro, P. A. and Savoie, D. L.: A global three-dimensional model of tropospheric sulfate, J. Geophys. Res. Atmos., 101(D13), 18667–18690, doi:10.1029/96JD01221, 1996.

Draxler, R. R. and Hess, G. D.: Description of the HYSPLIT_4 modeling system, Tech. Rep. NOAA Technical Memo ERL ARL-224, Silver Spring, Maryland, USA., 1997.

Draxler, R. R. and Hess, G. D.: An overview of the HYSPLIT 4 modelling system for trajectories, dispersion and deposition, Aust. Met. Mag., 47(4), 295–308, 1998.

Drewnick, F., Hings, S. S., DeCarlo, P., Jayne, J. T., Gonin, M., Fuhrer, K., Weimer, S., Jimenez, J. L., Demerjian, K. L., Borrmann, S. and Worsnop, D. R.: A New Time-of-Flight Aerosol Mass Spectrometer (TOF-AMS)—Instrument Description and First Field Deployment, Aerosol Sci. Technol., 39(7), 637–658, doi:10.1080/02786820500182040, 2005.

Ebmeier, S. K., Sayer, A. M., Grainger, R. G., Mather, T. A. and Carboni, E.: Systematic satellite observations of the impact of aerosols from passive volcanic degassing on local cloud properties, Atmos. Chem. Phys., 14(19), 10601–10618, doi:10.5194/acp-14-10601-2014, 2014.

Eisinger, M. and Burrows, J. P.: Tropospheric sulfur dioxide observed by the ERS-2 GOME instrument, Geophys. Res. Lett., 25(22), 4177–4180, doi:10.1029/1998GL900128, 1998.

Galle, B., Oppenheimer, C., Geyer, A., McGonigle, A. J. ., Edmonds, M. and Horrocks, L.: A miniaturised ultraviolet spectrometer for remote sensing of SO2 fluxes: a new tool for volcano surveillance, J. Volcanol. Geotherm. Res., 119(1–4), 241–254, doi:10.1016/S0377-0273(02)00356-6, 2003.

Global Volcanism Program: Report on Nyamuragira (DR Congo), in Venzke, E (ed.), Bulletin of the Global Volcanism Network, 42:6. Smithsonian Institution., 2017.

van Hoek, M. and Claas, J.: Possibilities to avoid row anomaly rows Date Signature, TN-OMIE-KNMI-963, 2010.

Holanda, B. A., Wang, Q., Saturno, J., Ditas, F., Ditas, J., Pöhlker, M. L., Klimach, T., Moran-Zuloaga, D., Schulz, C., Ming, J., Cheng, Y., Su, H., Wendisch, M., Machado, L. A. T., Schneider, J., Pöhlker, C., Artaxo, P., Pöschl, U. and Andreae, M. O.: Transatlantic transport of pollution aerosol from Africa to the Amazon rain forest - Aircraft observations in the context of the ACRIDICON-CHUVA campaign, Atmos. Chem. Phys. Discuss., in preparation, 2017.

Ilyinskaya, E., Schmidt, A., Mather, T. A., Pope, F. D., Witham, C., Baxter, P., Jóhannsson, T., Pfeffer, M., Barsotti, S., Singh, A., Sanderson, P., Bergsson, B., McCormick Kilbride, B., Donovan, A., Peters, N., Oppenheimer, C. and Edmonds, M.: Understanding the environmental impacts of large fissure eruptions: Aerosol and gas emissions from the 2014–2015 Holuhraun eruption (Iceland), Earth Planet. Sci. Lett., 472, 309–322, doi:10.1016/j.epsl.2017.05.025, 2017.

Jardine, K., Yañez-Serrano, A. M., Williams, J., Kunert, N., Jardine, A., Taylor, T., Abrell, L., Artaxo, P., Guenther, A., Hewitt, C. N., House, E., Florentino, A. P., Manzi, A., Higuchi, N., Kesselmeier, J., Behrendt, T., Veres, P. R., Derstroff, B., Fuentes, J. D., Martin, S. T. and Andreae, M. O.: Dimethyl sulfide in the Amazon rain forest, Global Biogeochem. Cycles, 29(1), 19–32, doi:10.1002/2014GB004969, 2015.

Khodri, M., Izumo, T., Vialard, J., Janicot, S., Cassou, C., Lengaigne, M., Mignot, J., Gastineau, G., Guilyardi, E., Lebas, N., Robock, A. and McPhaden, M. J.: Tropical explosive volcanic eruptions can trigger El Niño by cooling tropical Africa, Nat. Commun., 8(1), 778, doi:10.1038/s41467-017-00755-6, 2017.

Khokhar, M. F., Frankenberg, C., Van Roozendael, M., Beirle, S., Kühl, S., Richter, A., Platt, U. and Wagner, T.: Satellite observations of atmospheric SO2 from volcanic eruptions during the time-period of 1996–2002, Adv. Sp. Res., 36(5), 879–887, doi:10.1016/j.asr.2005.04.114, 2005.

Kirchner, I., Stenchikov, G. L., Graf, H.-F., Robock, A. and Antuña, J. C.: Climate model simulation of winter warming and summer cooling following the 1991 Mount Pinatubo volcanic eruption, J. Geophys. Res. Atmos., 104(D16), 19039–19055, doi:10.1029/1999JD900213, 1999.

Kleist, D. T., Parrish, D. F., Derber, J. C., Treadon, R., Wu, W.-S., Lord, S., Kleist, D. T., Parrish, D. F., Derber, J. C., Treadon, R., Wu, W.-S. and Lord, S.: Introduction of the GSI into the NCEP Global Data Assimilation System, Weather Forecast., 24(6), 1691–1705, doi:10.1175/2009WAF2222201.1, 2009.



Krueger, A. J. and J., A.: Detection of volcanic eruptions from space by their sulfur dioxide clouds, Am. Inst. Aeronaut. Astronaut. Aerosp. Sci. Meet. 23rd, Reno, NV, Jan. 14-17, 1985. 5 p., 1985.

Kuhn, U., Ganzeveld, L., Thielmann, A., Dindorf, T., Schebeske, G., Welling, M., Sciare, J., Roberts, G., Meixner, F. X., Kesselmeier, J., Lelieveld, J., Kolle, O., Ciccioli, P., Lloyd, J., Trentmann, J., Artaxo, P. and Andreae, M. O.: Impact of Manaus City on the Amazon Green Ocean atmosphere: Ozone production, precursor sensitivity and aerosol load, Atmos. Chem. Phys., 10(19), 9251–9282, doi:10.5194/acp-10-9251-2010, 2010.

Levelt, P. F., van den Oord, G. H. J., Dobber, M. R., Malkki, A., Huib Visser, Johan de Vries, Stammes, P., Lundell, J. O. V. and Saari, H.: The ozone monitoring instrument, IEEE Trans. Geosci. Remote Sens., 44(5), 1093–1101, doi:10.1109/TGRS.2006.872333, 2006.

Li, C., Joiner, J., Krotkov, N. A. and Bhartia, P. K.: A fast and sensitive new satellite SO2 retrieval algorithm based on principal component analysis: Application to the ozone monitoring instrument, Geophys. Res. Lett., 40(23), 6314–6318, doi:10.1002/2013GL058134, 2013.

Li, C., Krotkov, N. A., Carn, S., Zhang, Y., Spurr, R. J. D. and Joiner, J.: New-generation NASA Aura Ozone Monitoring Instrument (OMI) volcanic SO2 dataset: algorithm description, initial results, and continuation with the Suomi-NPP Ozone Mapping and Profiler Suite (OMPS), Atmos. Meas. Tech., 10(2), 445–458, doi:10.5194/amt-10-445-2017, 2017.

Machado, L. A. T., Silva Dias, M. A. F., Morales, C., Fisch, G., Vila, D., Albrecht, R., Goodman, S. J., Calheiros, A. J. P., Biscaro, T., Kummerow, C., Cohen, J., Fitzjarrald, D., Nascimento, E. L., Sakamoto, M. S., Cunningham, C., Chaboureau, J.-P., Petersen, W. A., Adams, D. K., Baldini, L., Angelis, C. F., Sapucci, L. F., Salio, P., Barbosa, H. M. J., Landulfo, E., Souza, R. A. F., Blakeslee, R. J., Bailey, J., Freitas, S., Lima, W. F. A. and Tokay, A.: The Chuva Project: How Does Convection Vary across Brazil?, Bull. Am. Meteorol. Soc., 95(9), 1365–1380, doi:10.1175/BAMS-D-13-00084.1, 2014.

Malavelle, F. F., Haywood, J. M., Jones, A., Gettelman, A., Clarisse, L., Bauduin, S., Allan, R. P., Karset, I. H. H., Kristjánsson, J. E., Oreopoulos, L., Cho, N., Lee, D., Bellouin, N., Boucher, O., Grosvenor, D. P., Carslaw, K. S., Dhomse, S., Mann, G. W., Schmidt, A., Coe, H., Hartley, M. E., Dalvi, M., Hill, A. A., Johnson, B. T., Johnson, C. E., Knight, J. R., O'Connor, F. M., Partridge, D. G., Stier, P., Myhre, G., Platnick, S., Stephens, G. L., Takahashi, H. and Thordarson, T.: Strong constraints on aerosol–cloud interactions from volcanic eruptions, Nature, 546(7659), 485–491, doi:10.1038/nature22974, 2017.

Martin, S. T., Andreae, M. O., Artaxo, P., Baumgardner, D., Chen, Q., Goldstein, A. H., Guenther, A., Heald, C. L., Mayol-Bracero, O. L., McMurry, P. H., Pauliquevis, T., Pöschl, U., Prather, K. A., Roberts, G. C., Saleska, S. R., Silva Dias, M. A., Spracklen, D. V., Swietlicki, E. and Trebs, I.: Sources and properties of Amazonian aerosol particles, Rev. Geophys., 48(2), RG2002, doi:10.1029/2008RG000280, 2010.

Martin, S. T., Artaxo, P., Machado, L. A. T., Manzi, A. O., Souza, R. A. F., Schumacher, C., Wang, J., Andreae, M. O., Barbosa, H. M. J., Fan, J., Fisch, G., Goldstein, A. H., Guenther, A., Jimenez, J. L., Pöschl, U., Silva Dias, M. A., Smith, J. N. and Wendisch, M.: Introduction: Observations and Modeling of the Green Ocean Amazon (GoAmazon2014/5), Atmos. Chem. Phys., 16(8), 4785–4797, doi:10.5194/acp-16-4785-2016, 2016.

Martin, S. T., Artaxo, P., Machado, L., Manzi, A. O., Souza, R. A. F., Schumacher, C., Wang, J., Biscaro, T., Brito, J., Calheiros, A., Jardine, K., Medeiros, A., Portela, B., de Sá, S. S., Adachi, K., Aiken, A. C., Albrecht, R., Alexander, L., Andreae, M. O., Barbosa, H. M. J., Buseck, P., Chand, D., Comstock, J. M., Day, D. A., Dubey, M., Fan, J., Fast, J., Fisch, G., Fortner, E., Giangrande, S., Gilles, M., Goldstein, A. H., Guenther, A., Hubbe, J., Jensen, M., Jimenez, J. L., Keutsch, F. N., Kim, S., Kuang, C., Laskin, A., McKinney, K., Mei, F., Miller, M., Nascimento, R., Pauliquevis, T., Pekour, M., Peres, J., Petäjä, T., Pöhlker, C., Pöschl, U., Rizzo, L., Schmid, B., Shilling, J. E., Dias, M. A. S., Smith, J. N., Tomlinson, J. M., Tóta, J. and Wendisch, M.: The Green Ocean Amazon Experiment (GoAmazon2014/5) Observes Pollution Affecting Gases, Aerosols, Clouds, and Rainfall over the Rain Forest, Bull. Am. Meteorol. Soc., 98(5), 981–997, doi:10.1175/BAMS-D-15-00221.1, 2017.

Mather, T. A., Pyle, D. M. M. and Oppenheimer, C.: Tropospheric volcanic aerosol, in Volcanism Earth's atmosphere, pp. 189–212., 2003.

McNaughton, C. S., Clarke, A. D., Freitag, S., Kapustin, V. N., Kondo, Y., Moteki, N., Sahu, L., Takegawa, N., Schwarz, J. P., Spackman, J. R., Watts, L., Diskin, G., Podolske, J., Holloway, J. S., Wisthaler, A., Mikoviny, T., De Gouw, J., Warneke, C., Jimenez, J., Cubison, M., Howell, S. G., Middlebrook, A., Bahreini, R., Anderson, B. E., Winstead, E., Thornhill, K. L., Lack, D., Cozic, J. and Brock, C. A.: Absorbing aerosol in the troposphere of the Western Arctic during the 2008 ARCTAS/ARCPAC airborne field campaigns, Atmos. Chem. Phys., 11(15), 7561–7582, doi:10.5194/acp-11-7561-2011, 2011.

Müller, T., Laborde, M., Kassell, G. and Wiedensohler, A.: Design and performance of a three-wavelength LED-based total scatter and backscatter integrating nephelometer, Atmos. Meas. Tech., 4(6), 1291–1303, doi:10.5194/amt-4-1291-2011, 2011.

Ng, N. L., Herndon, S. C., Trimborn, A., Canagaratna, M. R., Croteau, P. L., Onasch, T. B., Sueper, D., Worsnop, D. R., Zhang, Q., Sun, Y. L. and Jayne, J. T.: An Aerosol Chemical Speciation Monitor (ACSM) for Routine Monitoring of the Composition and Mass Concentrations of Ambient Aerosol, Aerosol Sci. Technol., 45(7), 780–794, doi:10.1080/02786826.2011.560211, 2011.

Petzold, A. and Schönlinner, M.: Multi-angle absorption photometry—a new method for the measurement of aerosol light absorption and atmospheric black carbon, J. Aerosol Sci., 35(4), 421–441, doi:10.1016/j.jaerosci.2003.09.005, 2004.

Platt, U. and Stutz, J. (Jochen): Differential optical absorption spectroscopy : principles and applications, Springer Verlag., 2008.

Pöhlker, C., Walter, D., Paulsen, H., Könemann, T., Moran-Zuloaga, D., Pickersgill, D., Ditas, F., Saturno, J., Lammel, G., Després, V. R., Artaxo, P. and Andreae, M. O.: Technical Note: Back trajectory analysis, land cover footprints, and future perturbation trends in the upwind fetch of the ATTO site in the central Amazon, Atmos. Chem. Phys. Discuss., in preparation, 2017a.

Pöhlker, M. L., Pöhlker, C., Ditas, F., Klimach, T., Hrabe de Angelis, I., Araújo, A., Brito, J., Carbone, S., Cheng, Y., Chi, X., Ditz, R., Gunthe, S. S., Kesselmeier, J., Könemann, T., Lavrič, J. V., Martin, S. T., Mikhailov, E., Moran-Zuloaga, D., Rose, D., Saturno, J., Su, H., Thalman, R., Walter, D., Wang, J., Wolff, S., Barbosa, H. M. J., Artaxo, P., Andreae, M. O. and Pöschl, U.: Long-term observations of cloud condensation nuclei in the Amazon rain forest – Part 1: Aerosol size distribution, hygroscopicity, and new model parametrizations for CCN prediction, Atmos. Chem. Phys., 16(24), 15709–15740, doi:10.5194/acp-16-15709-2016, 2016.

Pöhlker, M. L., Ditas, F., Saturno, J., Klimach, T., Hrabě de Angelis, I., Araùjo, A., Brito, J., Carbone, S., Cheng, Y., Chi, X., Ditz, R., Gunthe, S. S., Kandler, K., Kesselmeier, J., Könemann, T., Lavrič, J. V., Martin, S. T., Mikhailov, E., Moran-Zuloaga, D., Rizzo, L. V., Rose, D., Su, H., Thalman, R., Walter, D., Wang, J., Wolff, S., Barbosa, H. M. J., Artaxo, P., Andreae, M. O., Pöschl, U. and Pöhlker, C.: Long-term observations of cloud condensation nuclei in the Amazon rain forest - Part 2: Variability and characteristic differences under near-pristine, biomass burning, and long-range transport conditions, Atmos. Chem. Phys. Discuss., 1–51, doi:10.5194/acp-2017-847, 2017b.

Reiner, T. and Arnold, F.: Laboratory investigations of gaseous sulfuric acid formation via SO 3 +H 2 O+M→H 2 SO 4 +M: Measurement of the rate constant and product identification, J. Chem. Phys., 101(9), 7399–7407, doi:10.1063/1.468298, 1994.

Richter, A. and Wagner, T.: The Use of UV, Visible and Near IR Solar Back Scattered Radiation to Determine Trace Gases, in The Remote Sensing of Tropospheric Composition from Space, Physics of Earth and Space Environments, ISBN 978-3-642-14790-6. Springer-Verlag Berlin Heidelberg, 2011, p. 67, edited by J. P. Burrows, P. Borrell, and U. Platt, pp. 67–121., 2011.

de Sá, S. S., Palm, B. B., Campuzano-Jost, P., Day, D. A., Newburn, M. K., Hu, W., Isaacman-VanWertz, G., Yee, L. D., Thalman, R., Brito, J., Carbone, S., Artaxo, P., Goldstein, A. H., Manzi, A. O., Souza, R. A. F., Mei, F., Shilling, J. E., Springston, S. R., Wang, J., Surratt, J. D., Alexander, M. L., Jimenez, J. L. and Martin, S. T.: Influence of urban pollution on the production of organic particulate matter from isoprene epoxydiols in central Amazonia, Atmos. Chem. Phys., 17(11), 6611–6629, doi:10.5194/acp-17-6611-2017, 2017.

Saturno, J., Holanda, B. A., Pöhlker, C., Ditas, F., Wang, Q., Morán-Zuloaga, D., Brito, J., Carbone, S., Cheng, Y., Chi, X., Ditas, J., Hoffmann, T., Hrabě de Angelis, I., Könemann, T., Lavrič, J. V., Ma, N., Ming, J., Paulsen, H., Pöhlker, M. L., Rizzo, L. V., Schlag, P., Su, H., Walter, D., Wolff, S., Zhang, Y., Artaxo, P., Pöschl, U. and Andreae, M. O.: Black and brown carbon over central Amazonia: Long-term aerosol measurements at the ATTO site, Atmos. Chem. Phys. Discuss., submitted, 2017.

Stein, A. F., Draxler, R. R., Rolph, G. D., Stunder, B. J. B., Cohen, M. D. and Ngan, F.: NOAA's HYSPLIT Atmospheric Transport and Dispersion Modeling System, Bull. Am. Meteorol. Soc., 96(12), 2059–2077, doi:10.1175/BAMS-D-14-00110.1, 2015.

Stephens, M., Turner, N. and Sandberg, J.: Particle Identification by Laser-Induced Incandescence in a Solid-State Laser Cavity, Appl. Opt., 42(19), 3726, doi:10.1364/AO.42.003726, 2003.

Stevens, B. and Feingold, G.: Untangling aerosol effects on clouds and precipitation in a buffered system., Nature, 461(7264), 607–613, doi:10.1038/nature08281, 2009.

Talbot, R. W., Andreae, M. O., Andreae, T. W. and Harriss, R. C.: Regional aerosol chemistry of the Amazon Basin during the dry season, J. Geophys. Res., 93(D2), 1499, doi:10.1029/JD093iD02p01499, 1988.

Wang, Q., Saturno, J., Chi, X., Walter, D., Lavric, J. V., Moran-Zuloaga, D., Ditas, F., Pöhlker, C., Brito, J., Carbone, S., Artaxo, P. and Andreae, M. O.: Modeling investigation of light-absorbing aerosols in the Amazon Basin during the wet season, Atmos. Chem. Phys., 16(22), 14775–14794, doi:10.5194/acp-16-14775-2016, 2016.

Wendisch, M., Pöschl, U., Andreae, M. O., Machado, L. A. T., Albrecht, R., Schlager, H., Rosenfeld, D., Martin, S. T., Abdelmonem, A., Afchine, A., Araùjo, A. C., Artaxo, P., Aufmhoff, H.,

Barbosa, H. M. J., Borrmann, S., Braga, R., Buchholz, B., Cecchini, M. A., Costa, A., Curtius, J., Dollner, M., Dorf, M., Dreiling, V., Ebert, V., Ehrlich, A., Ewald, F., Fisch, G., Fix, A., Frank, F., Fütterer, D., Heckl, C., Heidelberg, F., Hüneke, T., Jäkel, E., Järvinen, E., Jurkat, T., Kanter, S., Kästner, U., Kenntner, M., Kesselmeier, J., Klimach, T., Knecht, M., Kohl, R., Kölling, T., Krämer, M., Krüger, M., Krisna, T. C., Lavric, J. V., Longo, K., Mahnke, C., Manzi, A. O., Mayer, B., Mertes, S., Minikin, A., Molleker, S., Münch, S., Nillius, B., Pfeilsticker, K., Pöhlker, C., Roiger, A., Rose, D., Rosenow, D., Sauer, D., Schnaiter, M., Schneider, J., Schulz, C., de Souza, R. A. F., Spanu, A., Stock, P., Vila, D., Voigt, C., Walser, A., Walter, D., Weigel, R., Weinzierl, B., Werner, F., Yamasoe, M. A., Ziereis, H., Zinner, T. and Zöger, M.: ACRIDICON–CHUVA Campaign: Studying Tropical Deep Convective Clouds and Precipitation over Amazonia Using the New German Research Aircraft HALO, Bull. Am. Meteorol. Soc., 97(10), 1885–1908, doi:10.1175/BAMS-D-14-00255.1, 2016.

Yang, Y., Wang, H., Smith, S. J., Easter, R., Ma, P., Qian, Y., Yu, H., Li, C. and Rasch, P. J.: Global source attribution of sulfate concentration and direct and indirect radiative forcing, Atmos. Chem. Phys., 17(14), 8903–8922, doi:10.5194/acp-17-8903-2017, 2017.

Yuan, T., Remer, L. A. and Yu, H.: Microphysical, macrophysical and radiative signatures of volcanic aerosols in trade wind cumulus observed by the A-Train, Atmos. Chem. Phys., 11(14), 7119–7132, doi:10.5194/acp-11-7119-2011, 2011.

Atmos. Chem. Phys. Discuss., https://doi.org/10.5194/acp-2017-1152
Manuscript under review for journal Atmos. Chem. Phys.
Discussion started: 15 December 2017


Atmospheric Chemistry and Physics Discussions

**Table 1.** Measurements at points along track of the flight AC14 (21 September 2014) selected as starting points for backward trajectories presented in Fig. 6. Data points with sulfate-to-OA > 1 are emphasized by bold font.

| Time (UTC) | Latitude [°N] | Longitude [°E] | Altitude [km] | $M_{sulfate}$ [μg $m^{-3}$] | Sulfate-to-OA | Color in Fig. 6 |
|---|---|---|---|---|---|---|
| 15:14 | -2.75 | -60.34 | 1.61 | 1.2 | 0.5 | Gray |
| **16:19** | **-3.19** | **-60.21** | **4.50** | **1.0** | **1.1** | **Blue** |
| **16:36** | **-4.00** | **-59.50** | **4.50** | **3.0** | **2.9** | **Green** |
| **16:54** | **-5.20** | **-59.25** | **4.49** | **3.1** | **7.8** | **Red** |
| 17:11 | -6.45 | -58.98 | 6.45 | 0.6 | 0.8 | Gray |
| 17:46 | -4.52 | -59.40 | 6.43 | 0.5 | 0.8 | Gray |
| 19:40 | -4.44 | -59.41 | 7.68 | 1.2 | 1.0 | Gray |
| **21:41** | **-3.79** | **-59.55** | **4.79** | **1.8** | **2.2** | **Light blue** |
| 21:59 | -3.04 | -60.20 | 0.90 | 1.2 | 0.3 | Gray |

Atmos. Chem. Phys. Discuss., https://doi.org/10.5194/acp-2017-1152
Manuscript under review for journal Atmos. Chem. Phys.
Discussion started: 15 December 2017


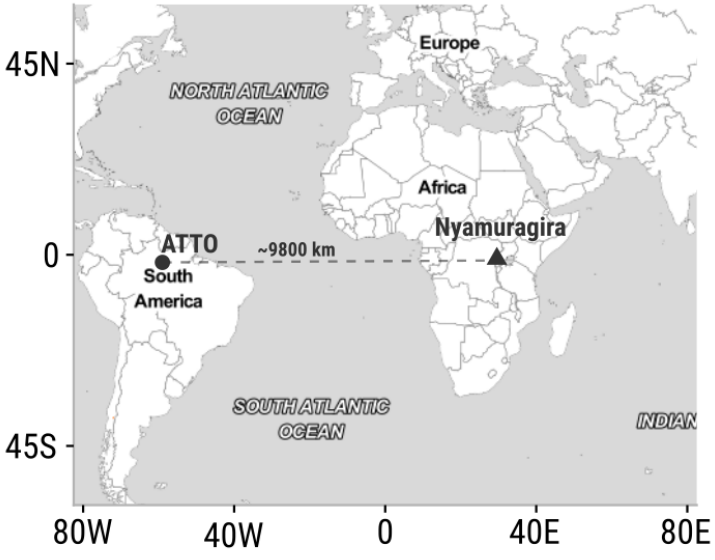


**Figure 1.** ATTO site and Nyamuragira volcano locations.

Atmos. Chem. Phys. Discuss., https://doi.org/10.5194/acp-2017-1152
Manuscript under review for journal Atmos. Chem. Phys.
Discussion started: 15 December 2017


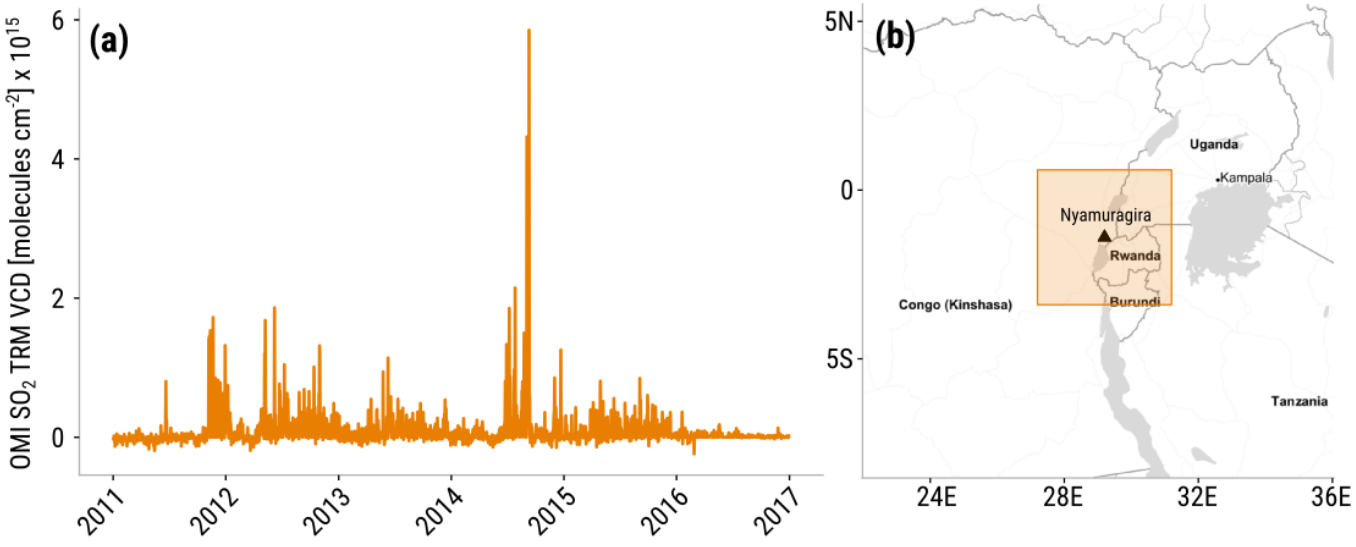


**Figure 2.** (a) Time series of daily-averaged OMI $SO_2$ TRM VCD observations corresponding to the averages over the area delimited by 27.2° E, 3.4° S, 31.2° E, and 0.6° N (b). Map of eastern Africa showing the averaging area (orange square). The location of Nyamuragira is represented by a black triangle.

Atmos. Chem. Phys. Discuss., https://doi.org/10.5194/acp-2017-1152
Manuscript under review for journal Atmos. Chem. Phys.
Discussion started: 15 December 2017


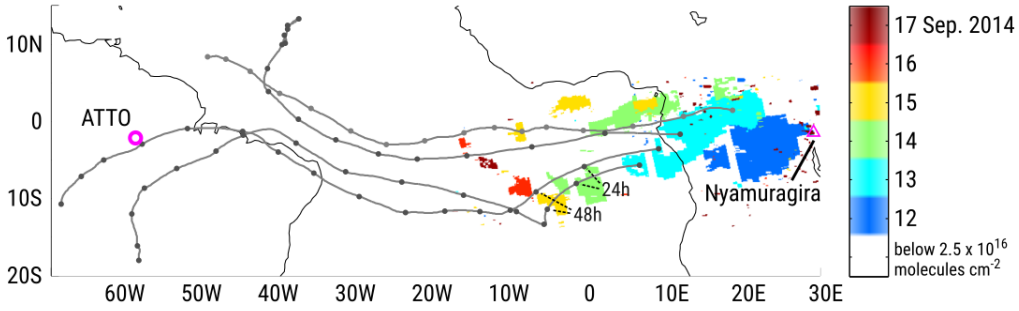


**Figure 3.** Map of $SO_2$ plumes with VCD > $2.5 \times 10^{16}$ molecules $cm^{-2}$ color-coded by date of observation. Forward trajectories started at 4 km (above mean sea level, a.m.s.l.) at four locations within the plume detected on 13 September 2014 (light blue) are indicated by black lines with markers at 24-hour intervals. The ATTO site is marked by a pink circle; the location of Nyamuragira is indicated by a pink triangle.

Atmos. Chem. Phys. Discuss., https://doi.org/10.5194/acp-2017-1152
Manuscript under review for journal Atmos. Chem. Phys.
Discussion started: 15 December 2017


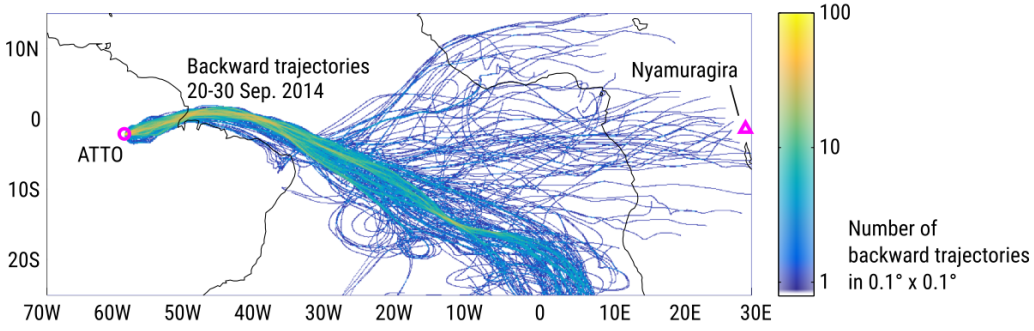


**Figure 4.** Density of backward trajectories started from ATTO at an altitude of 300 m a.m.s.l. on every hour starting at 0:00 UTC on 20 September 2014 up to 23:00 UTC on 30 September 2014. The locations of the ATTO site and Nyamuragira are shown on the map.

Atmos. Chem. Phys. Discuss., https://doi.org/10.5194/acp-2017-1152
Manuscript under review for journal Atmos. Chem. Phys.
Discussion started: 15 December 2017


Atmospheric Chemistry and Physics Discussions

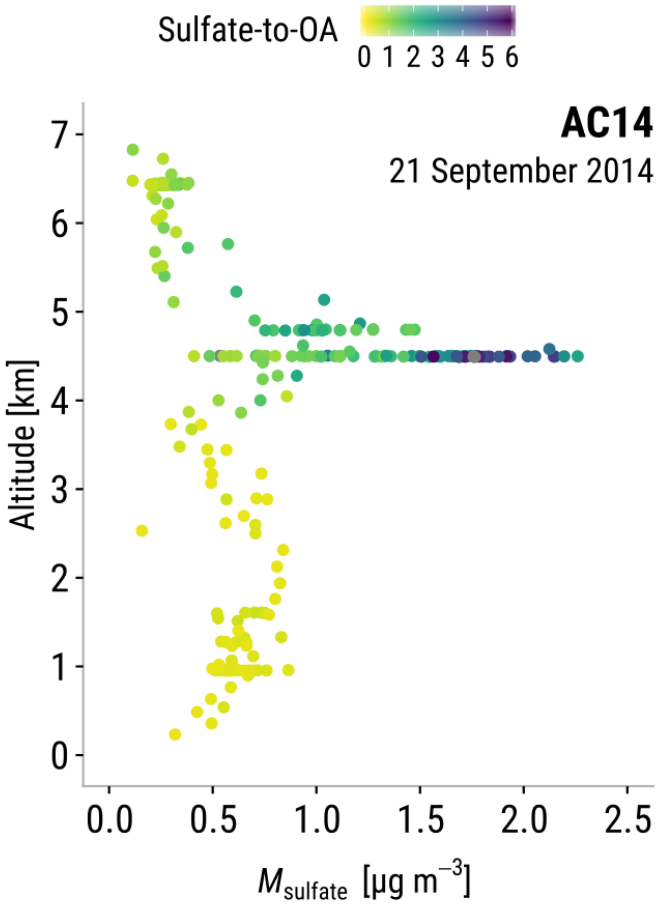


**Figure 5.** Sulfate layer observations over the Amazon rain forest. The figure shows the $M_{sulfate}$ vertical profile observed during flight AC14 (21 September 2014). Color-coded sulfate-to-OA values are truncated at a maximum of 6.

Atmos. Chem. Phys. Discuss., https://doi.org/10.5194/acp-2017-1152
Manuscript under review for journal Atmos. Chem. Phys.
Discussion started: 15 December 2017


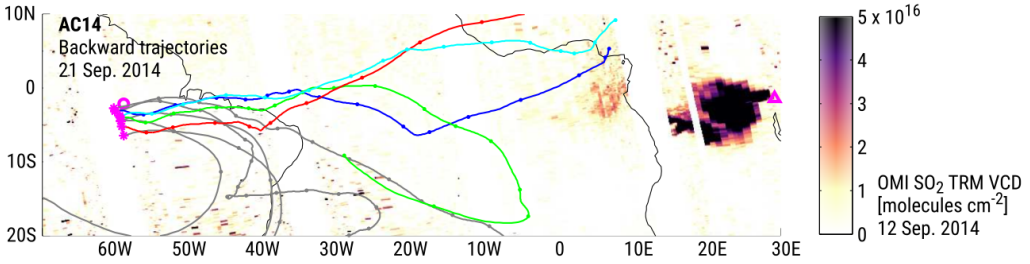


**Figure 6.** Map of gridded OMI $SO_2$ VCD, observed on 12 September 2014. Backward trajectories were started at several points along track of the flight AC14 (21 September 2014) at flight altitude. Trajectories starting at points where sulfate-to-OA > 1 are shown in color (see Table 1 for details), all other trajectories are shown in gray; dots are placed at 24-hour intervals. The path of flight AC14 is marked in pink, with stars denoting the starting points of the backward trajectories. The locations of the ATTO site and Nyamuragira are marked with a pink circle and triangle, respectively.

Atmos. Chem. Phys. Discuss., https://doi.org/10.5194/acp-2017-1152
Manuscript under review for journal Atmos. Chem. Phys.
Discussion started: 15 December 2017


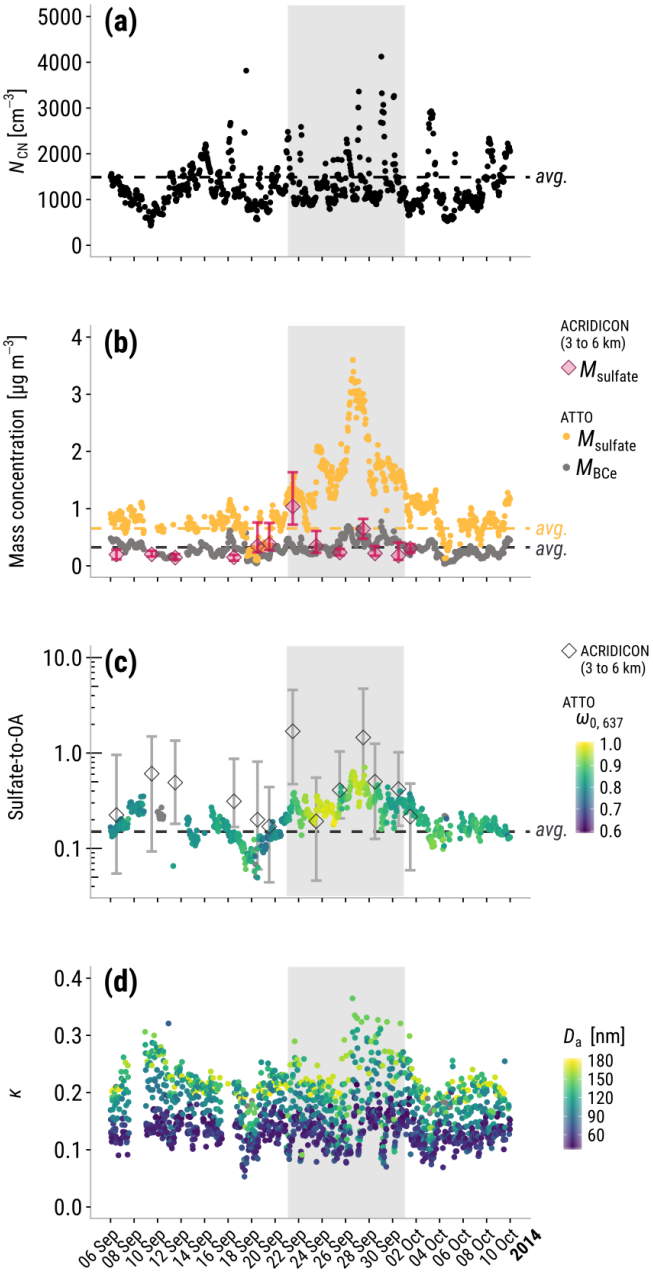


**Figure 7.** Different aerosol properties measured during the Nya2014 event (gray shaded area), These time series include ATTO hourly averages of (a) aerosol particle number concentration, $N_{CN}$, (b) sulfate and $BC_e$ mass concentration, (c) sulfate-to-OA mass ratio with color-coded aerosol particle single scattering albedo at 637 nm wavelength, and (d) hygroscopicity parameter, $\kappa$, original time resolution, with color-coded particle activation diameter. Dry season averages are shown as dashed lines. ACRIDICON-CHUVA flight medians and inter-quartile ranges from 3 to 6 km altitude are shown in (b) and (c).